JOURNAL PRE-PROOF

This is an early version of the article, published prior to copyediting, typesetting, and editorial correction. The manuscript has been accepted for publication and is now available online to ensure early dissemination, author visibility, and citation tracking prior to the formal issue publication.

It has not undergone final language verification, formatting, or technical editing by the journal's editorial team. Content is subject to change in the final Version of Record.

To differentiate this version, it is marked as "PRE-PROOF PUBLICATION" and should be cited with the provided DOI. A visible watermark on each page indicates its preliminary status.

The final version will appear in a regular issue of *Archives of Acoustics*, with final metadata, layout, and pagination.

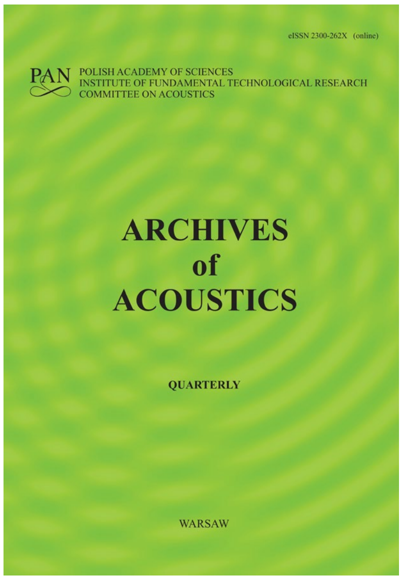

Title: Experimental verification of the usefulness of G-weighted level in the assessment of infrasound noise from a wind farm

Author(s): Dominik Mleczko, Tadeusz Wszołek, Paweł Pawlik, Paweł Małecki, Bartłomiej Stępień, Maciej Kłaczyński

DOI: https://doi.org/10.24423/archacoust.2026.4523

Journal: *Archives of Acoustics*

ISSN: 0137-5075, e-ISSN: 2300-262X

Publication status: In press

Received: 2026-06-10

Accepted: 2026-07-30

Published pre-proof: 2026-08-24

Please cite this article as:

Mleczko D., Wszołek T., Pawlik P., Małecki P., Stępień B., Kłaczyński M. (2026), Experimental verification of the usefulness of G-weighted level in the assessment of infrasound noise from a wind farm, *Archives of Acoustics*, https://doi.org/10.24423/archacoust.2026.4523

Experimental verification of the usefulness of G-weighted level in the assessment of infrasound noise from a wind farm

Dominik Mleczko, Tadeusz Wszołek, Paweł Pawlik, Paweł Małecki, Bartłomiej Stępień, Maciej Kłaczyński*

Email addresses: dmleczko@agh.edu.pl[1]*, twszolek@agh.edu.pl[1], pawlik@agh.edu.pl[1], pawel.malecki@agh.edu.pl[1], bartlomiej.stepien@agh.edu.pl[1], mklaczyn@agh.edu.pl[1]

*Corresponding author

[1]AGH University of Krakow, Faculty of Mechanical Engineering and Robotics, al. Adama Mickiewicza 30, 30-059 Krakow, Poland

Keywords: infrasound noise, wind turbines, G-weighted level, microphone height, wind shielding, environmental noise measurement

Abstract

Environmental assessments of wind turbine noise commonly use microphone heights of 1.5 m or 4 m above ground level, whereas wind turbine measurement standards recommend ground-level measurements on a board to reduce wind-induced interference. This study addresses this methodological uncertainty by comparing four microphone configurations under identical in-situ conditions and relating the obtained indicators to turbine operating parameters. Measurements were performed 250 m downwind of a 2 MW Vestas V90 turbine for four configurations: board-mounted microphones with single and double windscreens, and tripod-mounted microphones at 1.5 m and 4 m above ground level. The analysis focused on G-weighted sound pressure levels and their relationship with wind speed, rotor speed and electrical power. The board-mounted configuration with a double windscreen produced the most stable time series and showed the strongest relationship with turbine operation, while being less sensitive to local near-ground wind variability than the elevated configurations. The results support the use of enhanced board-mounted wind protection for robust in-situ assessment of wind turbine infrasound.

1 Introduction

Wind turbines are a source of sound over a very broad frequency range, including the infrasound band (< 20 Hz). This issue has been investigated for many years, from early studies on wind turbine acoustics (Hubbard and Shepherd, 1990) to later reviews and reports summarising research findings from different countries (Rogers and Manwell, 2004; Tachibana, 2014). Previous studies have shown that, at distances typical of residential locations relative to wind turbines (from several hundred metres to several kilometres), infrasound levels remain well below the threshold of human hearing, as confirmed by both field measurements and theoretical analyses (Jakobsen, 2005). Despite this, infrasound remains a subject of research interest, primarily because of the methodological difficulties associated with its reliable measurement under environmental conditions. More broadly, infrasound forms part of the wider issue of low-frequency noise, the definitions and assessment context of which have been extensively discussed in the literature (Leventhall, Pelmear and Benton, 2003; Leventhall, 2009).

Interest in field measurements also stems from the fact that wind turbine noise is sometimes the subject of residents' complaints, as well as studies on annoyance and physiological responses, in which the role of low-frequency and infrasonic components is often considered (Baliatsas *et al.*, 2016; Pohl, Gabriel and Hübner, 2018; van Kamp and van den Berg, 2018; Gaßner *et al.*, 2022; Liebich *et al.*, 2022; Müller *et al.*, 2023). Regardless of differences in interpretation of these findings, from a measurement engineering perspective, the key issue remains the provision of a reliable and repeatable method for signal acquisition under environmental conditions. In practice, one of the major challenges in assessing the impact of wind farms is the separation of turbine emission from the background, dependent on wind speed, as already emphasised in classical methodological documents concerning wind farm noise assessment (Department of Trade and Industry, 1996).

One of the key problems in field infrasound measurements is the strong influence of wind-induced noise at the microphone (so-called pseudo-noise). The interaction of airflow with microphone components produces pressure fluctuations that are not acoustic waves in nature but are registered by the sensor as an infrasonic signal. Consequently, the observed levels within the infrasound band may largely reflect flow and turbulence conditions rather than the actual acoustic emission of the wind turbine, as widely described in the literature on wind-induced microphone noise (van den Berg, 2006; Raspet, Yu and Webster, 2008). Within the recorded infrasound band, turbine-related components, natural environmental background, and flow-induced artefacts generated at the microphone are superimposed, and their relative contributions may strongly depend on wind and propagation conditions (Møller and Pedersen, 2011; Hansen and Hansen, 2020; Nguyen *et al.*, 2022). At the same time, the literature also reports measurements of infrasonic components in wind turbine noise obtained using different experimental approaches, further highlighting the importance of the selected method and measurement configuration in field conditions (Boczar *et al.*, 2022). For this reason, the choice of measurement configuration is crucial for limiting the contribution of pseudo-noise and for the correct interpretation L_G values.

In measurement practice, infrasound is assessed using the G-weighted sound pressure level, as defined in ISO 7196. The G-weighting curve is characterised by amplification in the central part of the infrasound band, approximately within the range of 10–20 Hz. Frequencies below and above this range are progressively attenuated, although substantial attenuation only occurs above approximately 30–40 Hz. This means that the L_G indicator does not describe low-frequency noise in the range 20–200 Hz, but relates exclusively to infrasonic components. Consequently, L_G is particularly sensitive to all signal components occurring in the infrasound band, regardless of their origin (turbine emission versus pseudo-noise). Therefore, the $L_G$value may depend to a considerable extent on the contribution of wind-induced microphone noise and on the positioning and shielding of the microphone, rather than solely on the actual infrasonic emission of the turbine.

To reduce the influence of wind on the microphone, several solutions are used in practice, including large-diameter windshields, aerodynamic screens, and ground-based plates, as recommended in IEC/ISO 61400-11. Numerous solutions designed to reduce wind effects at the microphone, such as secondary windshields, domes, and multilayer structures, have been proposed and verified in the literature, although their effectiveness depends on both the frequency range and field conditions (Rogers and Manwell, 2004; Hansen, Zajamšek and Hansen, 2013; Hansen, Zajamsek and Hansen, 2014; Tachibana, 2014; D'Amico, Van Renterghem and Botteldooren, 2021; Wszołek, Pawlik, *et al.*, 2022; Rust and Koch, 2024). At the same time, approaches related to microphone height correction and to the assessment of discrepancies between measurements performed on a ground plate and at standard heights have also been developed, particularly under long-range propagation conditions (Kłaczyński and Wszołek, 2014; Hansen, Zajamšek and Hansen, 2019; Chiu and Lung, 2020). Despite the use of these solutions, in-situ infrasound measurements often exhibit considerable scatter, owing to L_G's high sensitivity to wind conditions and to the microphone's mounting and shielding. In many publications, only single-microphone configurations are analysed, or measurements are carried out under different environmental conditions, which makes direct comparison of results difficult. Relatively few studies assess different microphone configurations in parallel, that is, at the same time and under identical environmental conditions, while also quantitatively relating the results to wind turbine operating parameters. The principal novelty of the present study lies in the comparative analysis of four measurement configurations with different aerodynamic exposure (ground plate versus tripod; single versus double windshield), carried out in parallel under identical field conditions, and in the identification of those arrangements that provide the most stable and most "turbine-dependent" variation of L_G under changing wind conditions. Moreover, the obtained time histories were compared with turbine operating parameters obtained from the supervisory control and data acquisition (SCADA) system, namely rotational speed and generated power, to assess the extent to which L_G values reflect changes in the turbine operating state.

In the present study, the primary subject of analysis is infrasound assessed on the basis of the L_G level. The L_A level was retained as an auxiliary indicator facilitating the interpretation of changes related to turbine operating state and the distinction between these changes and those resulting from wind conditions. Variability in L_A may indicate changes in acoustic conditions in the vicinity of the microphone that favour the occurrence of pseudo-noise components affecting the L_G measurement. The parallel analysis of both indicators allows a clearer distinction between changes resulting from the turbine's actual noise emission and those caused by wind conditions and measurement configuration. One practical way of verifying whether the observed level variations are related to turbine operation is to compare the acoustic indicators with operational and meteorological parameters available from monitoring systems (SCADA), as well as wind measurements at different heights (Hansen, Zajamšek and Hansen, 2019; Wszołek *et al.*, 2020; Gaßner *et al.*, 2022). Such an approach allows distinguishing variability arising from turbine operation from that arising from flow conditions at the measurement location.

Consequently, according to the current state of knowledge, it has still not been unambiguously established to what extent the choice of microphone configuration affects the assessment of L_G in in-situ infrasound measurements, nor how the obtained values relate to wind turbine operating parameters, including wind speed at hub height, rotational speed, and power production. This study addresses this gap by means of a parallel assessment of four measurement configurations under identical field conditions and by quantitatively relating the obtained L_G and L_A levels to turbine operating parameters on the basis of correlation analysis.

2 Research Methods

2.1 Acoustic measurements

The measurements were designed to evaluate how microphone mounting height and windscreen configuration affect the reliability of G-weighted infrasound assessment near a wind turbine.

Sound pressure levels were recorded simultaneously on four channels using an SVAN 958 analyser and G.R.A.S. 40AZ microphones. Continuous acquisition was performed with 1 s resolution in 1/3-octave bands from 1 Hz to 20 kHz. Although the total recording time exceeded 4 h, the analysis was limited to 24 consecutive 10-min intervals. Short non-turbine-related disturbances, such as handling noise, nearby speech and occasional pass-by events, were identified in the 1 s time histories and excluded consistently from all four channels. Wind speed and direction at 1.5 m, 4 m and 10 m were measured using a meteorological mast located a few metres from the microphones and were synchronised with the acoustic data. Additional meteorological statistics are provided in Table 1A in Appendix A. Electrical power output data for the test turbine were obtained from the operator.

To analyse the impact of measurement configuration and microphone position on the noise measurement results, four measurement setups were used, as presented in Table 1.

Table 1 Measurement configurations used in the study.

Microphone mounting variant	Height (m)	Windscreen Type	Label
Ground plate + double windscreen (IEC/ISO 61400-11)	0	Double (90 mm + 500 mm hemispheres)	0m_DWS
Ground plate + single windscreen (IEC/ISO 61400-11)	0	Single (90 mm hemisphere)	0m_SWS
Tripod + single windscreen	1.5	Single (90 mm hemisphere)	1.5m_SWS
Tripod + single windscreen	4	Single (90 mm hemisphere)	4m_SWS

The selected configurations combine the ground-plate approach used in wind turbine sound power measurements according to IEC/ISO 61400-11 (IEC 61400-11, 2018), with microphone heights commonly used in environmental noise assessment. These include 1.5 m, as indicated in general acoustic assessment methodologies such as ISO 1996-2, and 4 m, used, among others, for measurement-based verification of computational models in strategic noise mapping (Directive 2002/49/EC).

2.2 Test turbine and measurement site conditions

The study was conducted near a Vestas V90 wind turbine with a rated power of 2 MW, a hub height of 105 m and a rotor diameter of 90 m. The cut-in, nominal and cut-out wind speeds are 4.0, 13.0 and 25.0 m/s, respectively. According to the manufacturer's data, the A-weighted sound power level increases from 94.4 dB at 4 m/s to 104.0 dB at 8 m/s (Vestas Wind Systems A/S, 2009).

Measurements were performed 250 m downwind of the test turbine, located at the edge of a wind farm consisting of 10 identical turbines (Fig. 1). During the analysed intervals, the wind direction was nearly constant, predominantly SE with rare short-term deviations towards ESE, which maintained downwind conditions relative to the test turbine and the wind farm. The remaining turbines were located 900–3000 m from the test turbine. Two operational scenarios were analysed: all turbines operating and only the test turbine operating, the latter providing a controlled dataset for correlation analysis.

The nearest road was approximately 350 m from the measurement site and had very low traffic volume; therefore, it was not expected to be a dominant source of interference. In cooperation with the wind farm operator, neighbouring turbines were temporarily stopped, and background measurements were performed with all turbines stopped. During the background measurements, wind speed ranged from 3 to 4 m/s, with gusts up to 6 m/s.

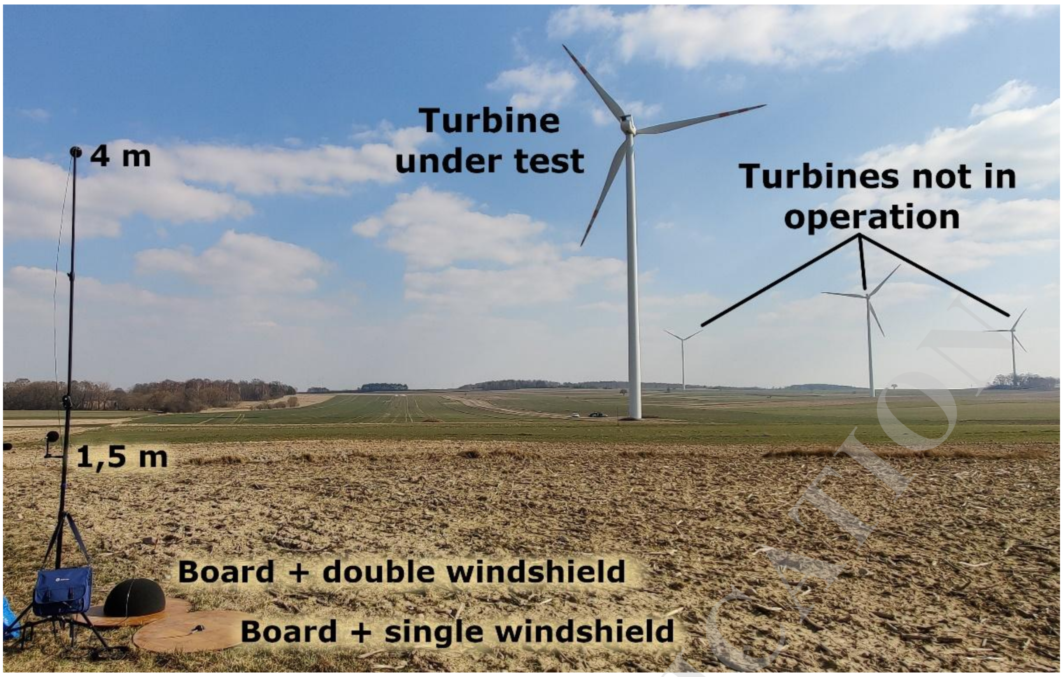

Fig. 1. Wind turbine under investigation and measurement point location.

2.3 Experiment description

Measurements were conducted on 17 March 2022 between 13:40 and 18:30 as part of the HETMAN project (Preis, 2021). Variable wind conditions during the campaign allowed noise levels to be recorded over a range of wind speeds.

The measurement scenarios are summarised in Table 2. The complete dataset for the 24 measurement intervals and the background measurements is provided in Table 2A in Appendix A. In the figures, the background level is shown as the mean of three consecutive 10-min intervals (BKG1–BKG3), whereas the individual background intervals are reported in Appendix A.

Table 2 Wind conditions and turbine operation during the analysed measurement intervals.

Measurement time	**Time frame no.**		**Wind speed at 1.5 m m/s**	**Wind speed at 4 m m/s**	**Wind speed at 10 m m/s**	**Wind speed at hub height m/s**
13:40 – 16:30	1 - 17	All turbines operating	Min 2.3 Max 5.6	Min 2.1 Max 5.2	Min 3.1 Max 7.3	Min 5.6 Max 7.9

16:30 – 17:00	18 – 24	One turbine only	Min 2.2 Max 2.8	Min 2.0 Max 2.5	Min 3.1 Max 4.0	Min 5.7 Max 7.9
18:00 – 18:30	BKG	No turbine operating	2.6	2.5	3.8	8.0

These synchronised acoustic, meteorological and operational data formed the basis for the correlation analysis described below.

2.4 Data Analysis Method

The recorded time histories of sound pressure levels in 1/3-octave bands were subjected to the following analysis:

a) The 1/3-octave band sound pressure level time series were segmented into 10-minute intervals.

b) For each interval, equivalent continuous sound pressure levels (L_{EQ}) were calculated for all 1/3-octave bands.

c) G-weighting (L_G) and A-weighting (L_A) were applied to the resulting 1/3-octave spectra.

d) Time series of the L_G and L_A were derived for 10-minute intervals.

The A- and G-weighted levels were calculated from the 1/3-octave-band spectra by applying the corresponding frequency-dependent weighting. For each 1/3-octave band with centre frequency f_i, the weighted band level was calculated as $L_{w,i} = L_i + C_w(f_i)$, where $L_i$is the unweighted band level and $C_w(f_i)$is the weighting in dB ($w \in \{A, G\}$). The overall weighted level was then computed by energy summation, $L_w = 10\log_{10}\left(\sum_i 10^{0.1L_{w,i}}\right)$. The A-weighting $C_A(f_i)$were taken from IEC 61672-1 and the G-weighting $C_G(f_i)$ from ISO 7196; the coefficient values used in this study are listed in Table 3.

Table 3 A- and G-weighting for 1/3-octave-band centre frequencies.

f, Hz	C_A(f), dB	C_G(f), dB	f, Hz	C_A(f), dB	C_G(f), dB
0.8	n/a	-49.5	20	-50.5	9
1	n/a	-43	25	-44.7	3.7
1.25	n/a	-37.5	31.5	-39.4	-4
1.6	n/a	-32.6	40	-34.6	-12
2	n/a	-28.3	50	-30.2	-20
2.5	n/a	-24.1	63	-26.6	-28
3.15	n/a	-20	80	-22.2	-36
4	n/a	-16	100	-19.1	-44

5	n/a	-12	125	-16.1	-52
6.3	n/a	-8	160	-13.4	-60
8	n/a	-4	200	-10.9	-68
10	-70.4	0	250	-8.8	-76
12.5	-63.4	4	315	-6.6	-84
16	-56.7	7.7			

Wind speed, acoustic indicators and turbine operational parameters were averaged over the same 10-min intervals. This interval length was adopted to ensure consistency with the SCADA data, which were available at 10-min resolution. Shorter acoustic windows were not used in the primary correlation analysis because they would require interpolation of turbine operating parameters or their exclusion from the analysis. This approach follows previous work on 10-min acoustic and operational parameter synchronisation (Wszołek, Mleczko, *et al.*, 2022).

Relationships between acoustic, meteorological and turbine operational parameters were evaluated using Pearson's linear correlation coefficient r. The analysis was based on a small sample of seven 10-min intervals for the single-turbine operating condition; therefore, the Shapiro–Wilk test was not used, as its reliability is limited for such small samples.

Correlations involving acoustic indicators (L_G, L_A) were calculated separately for each measurement configuration (0m_DWS, 0m_SWS, 1.5m_SWS and 4m_SWS). For each configuration, the following correlations were evaluated: $r(L_G, V_z)$ and $r(L_A, V_z)$, where V_z denotes the 10-min mean wind speed at $z \in \{1.5\text{ m}, 4\text{ m}, 10\text{ m}, \text{hub}\}$. Additionally, $r(L_G, L_A)$ was computed to assess the relationship between the two indicators. Correlations involving only meteorological and operational parameters (e.g., $r(V_{\text{hub}}, \text{Power})$, $r(V_{\text{hub}}, V_{10\text{ m}})$, $r(\text{TS}, \text{Power})$) were computed once per interval.

Two data subsets were used: intervals 1–17, with all turbines operating, and intervals 18–24, with only the test turbine operating. Correlations between acoustic indicators and wind speed were calculated for intervals 18–24 only, to relate the measured levels to a single, well-defined source. Correlations involving only meteorological and operational parameters were calculated using intervals 1–24.

3 Measurement results

The results are presented for all four measurement configurations. Particular attention is given to intervals 18–24, during which only the test turbine was operating. Background-corrected sound levels are shown in Figs. 2–5, with the BKG interval representing measurements with all turbines stopped. Detailed meteorological, operational and acoustic data are provided in Tables 1A and 2A in Appendix A.

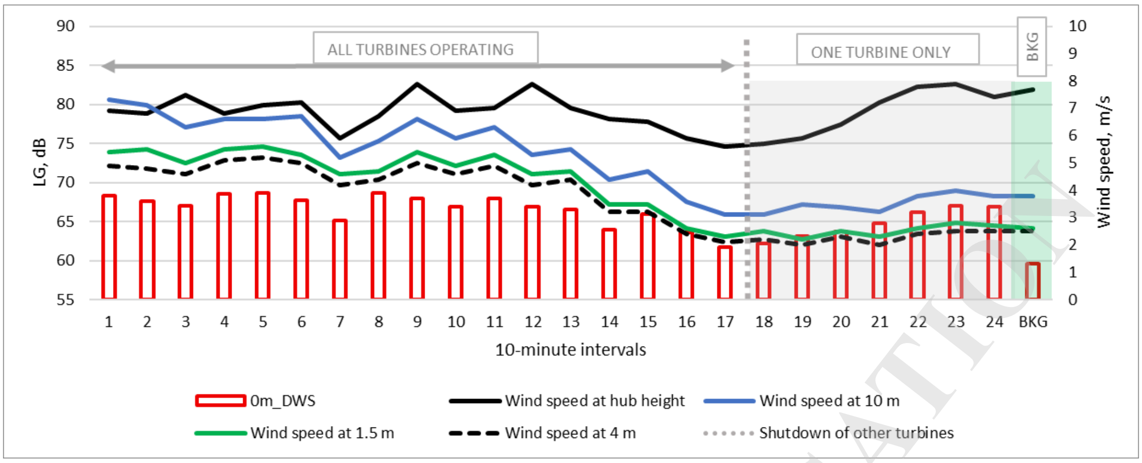

Fig. 2. G-weighted sound pressure level measured using the 0m_DWS configuration and wind speed recorded at hub height, 10 m, 4 m and 1.5 m a.g.l. across consecutive 10-min intervals.

Fig. 2 presents L_G for the 0m_DWS configuration together with wind speeds measured at hub height, 10 m, 4 m and 1.5 m a.g.l. From interval 18 onwards, hub-height wind speed increases, whereas near-ground wind speeds remain distinctly lower and show only minor fluctuations. The L_G trend follows hub-height wind speed, which is confirmed by the correlation coefficient $r(L_G, V_{hub}) = 0.96$; correlations with lower-level wind speeds are weaker (0.71–0.85).

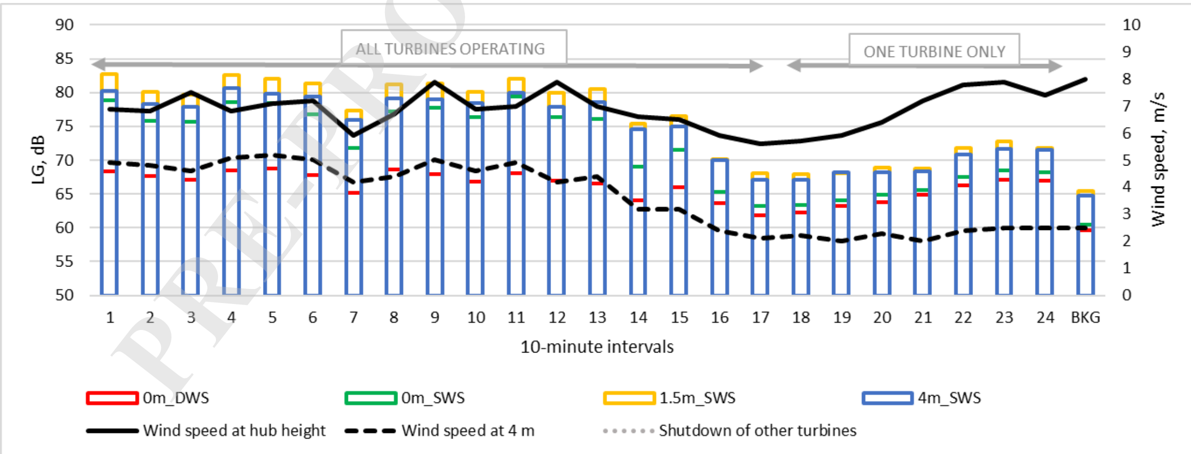

Fig. 3. G-weighted sound pressure levels measured using four microphone configurations and wind speed recorded at hub height and 4 m a.g.l. across consecutive 10-min intervals.

Fig. 3 compares L_G levels for all four microphone configurations. During intervals with higher near-ground wind speed, the 0m_DWS configuration gives clearly lower levels than the other setups, indicating lower susceptibility to wind-induced artefacts. In intervals 18–24, near-ground wind speed decreased while hub-height wind speed increased, resulting in more consistent L_G values across configurations. The high correlations with hub-height wind speed for the ground-plate configurations, $r = 0.96$ for 0m_DWS and $r = 0.95$ for 0m_SWS, confirm that these setups best reflect turbine-related changes under the analysed conditions.

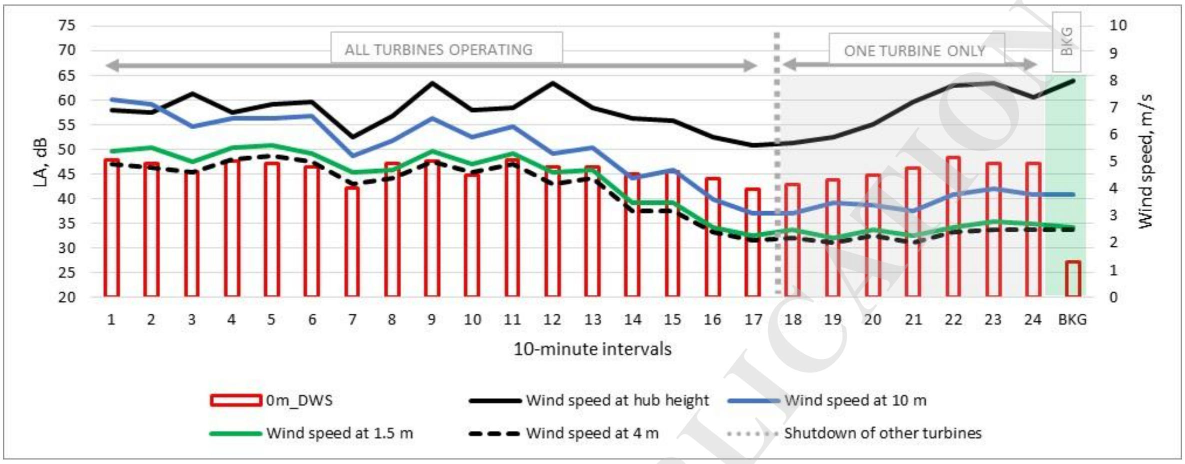

Fig. 4. A-weighted sound pressure level measured using the 0m_DWS configuration and wind speed recorded at hub height, 10 m, 4 m and 1.5 m a.g.l. across consecutive 10-min intervals.

Fig. 4 shows L_A for the 0m_DWS configuration together with wind speeds measured at all heights. During the single-turbine period, L_A is strongly related to hub-height wind speed, with $r(L_A, V_{hub}) = 0.97$. Owing to the strong attenuation of very low frequencies by A-weighting, $L_A$is less sensitive to infrasonic wind-induced pseudo-noise and is therefore used here as an auxiliary indicator of turbine-related trends.

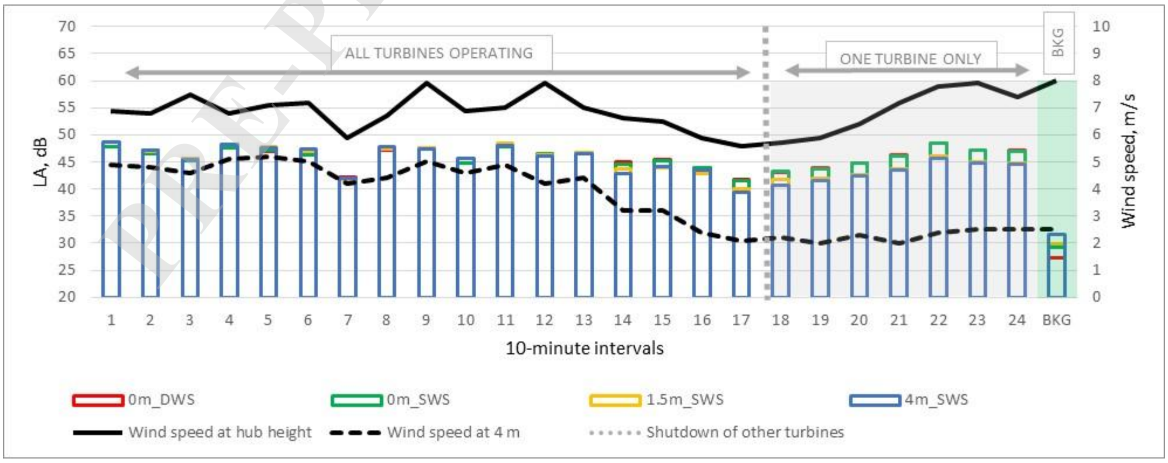

Fig. 5. A-weighted sound pressure levels measured using four microphone configurations and wind speed recorded at hub height and 4 m a.g.l. across consecutive 10-min intervals.

Fig. 5 compares L_A levels across all four configurations. In contrast to L_G, the differences between configurations are smaller, particularly during intervals with higher near-ground wind speed. Under lower wind conditions, slightly higher L_A values are observed for the ground-plate configurations, which may result from constructive interference between incident and reflected sound at the plate surface. Overall, A-weighting substantially reduces, but does not completely eliminate, the influence of wind-induced artefacts.

Fig. 6 compares 10-min wind speeds at 4 m a.g.l. and at hub height, together with the range of instantaneous fluctuations within each interval. The largest near-ground wind fluctuations occurred during the initial intervals, when increased variability of L_G was also observed for configurations with single windscreens.

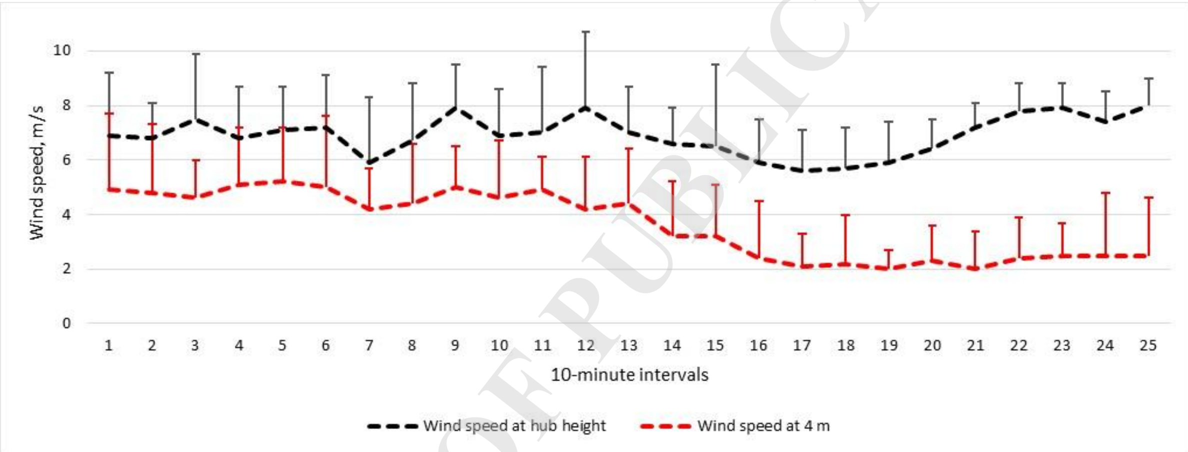

Fig. 6. Wind speed at 4 m a.g.l. and at hub height across consecutive 10-min intervals. Error bars indicate the range of instantaneous wind-speed fluctuations within each interval.

Fig. 7 shows the relationship between hub-height wind speed and average electrical power output, with data ordered by increasing wind speed for readability. A clear positive relationship is observed, with $R^2 = 0.951$, confirming that hub-height wind speed is a reliable proxy for turbine operating state. Some scatter remains, most likely due to short-term wind fluctuations and the dynamic response of the turbine.

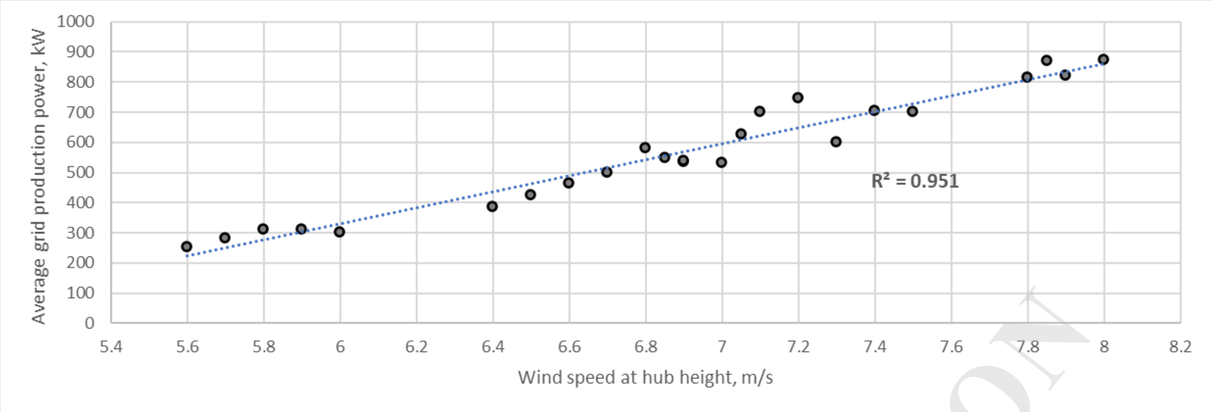

Fig. 7. Relationship between hub-height wind speed and average electrical power output of the test turbine in consecutive 10-min intervals.

Fig. 8 presents the relationship between turbine rotational speed and electrical power output. This relationship is also strong, with $R^2 = 0.904$, although slightly more scattered than the wind speed–power relationship. Rotational speed may therefore be used as an auxiliary operational parameter, while hub-height wind speed remains the more representative variable for interpreting acoustic trends.

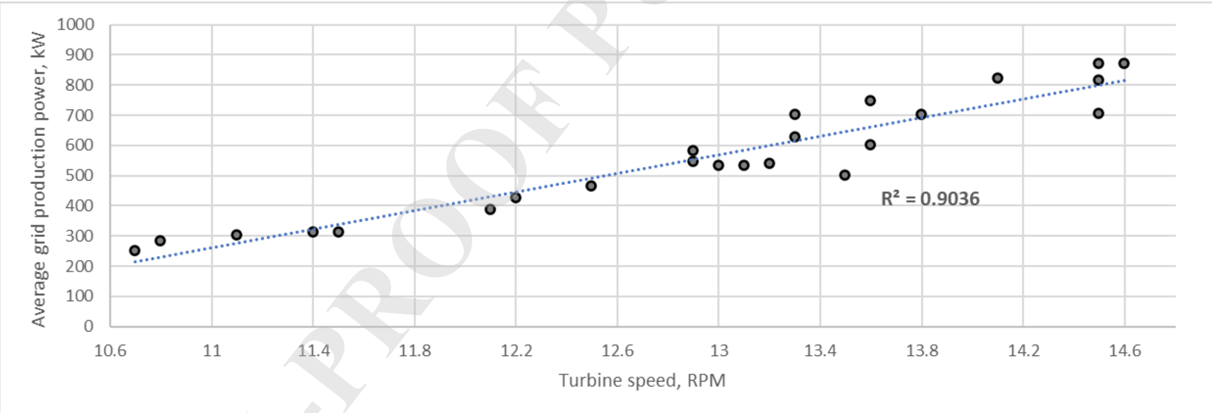

Fig. 8. Relationship between turbine rotational speed and average electrical power output in consecutive 10-min intervals.

4 Correlation Analysis

Table 4 summarises Pearson correlation coefficients between L_G and L_A sound levels, wind speeds near ground level and at hub height, and turbine operating parameters, including electrical power output and rotational speed. Despite the limited dataset of seven 10-min intervals, Pearson's coefficient was used, while normality testing was omitted due to its limited reliability for such small samples. Correlations involving L_G and L_A were calculated for intervals 18–24, during which only the test turbine was operating. This restriction was used to avoid contributions from neighbouring turbines and uncontrolled differences in propagation paths, which could distort the relationship between the measured sound levels and the test turbine's operating parameters. The coefficients were calculated separately for the four configurations: 0m_DWS, 0m_SWS, 1.5m_SWS and 4m_SWS.

Correlations independent of microphone configuration, i.e. V_{hub}–power, V_{hub}–V_{10m}, and turbine speed–power, were calculated using the full dataset (intervals 1–24), as they are not affected by neighbouring acoustic sources.

Table 4 Pearson correlation coefficients between acoustic indicators, wind speeds and turbine operating parameters.

	Measurement method	*0m_DWS*	*0m_SWS*	*1.5m_SWS*	*4m_SWS*
1)	*r(L_G,V_{hub})*	↑0.96	↑0.95	**↗0.90**	**↗0.88**
2)	*r(L_G,V_{10m})*	**↗0.85**	**↗0.88**	↑0.92	↑0.95
3)	*r(L_G, V_{4m})*	**↗0.72**	**↗0.77**	**↗0.86**	**↗0.81**
4)	*r(L_G, $V_{1.5m}$)*	**↗0.71**	**↗0.76**	**↗0.85**	**↗0.77**
5)	*r(L_A, V_{hub})*	↑0.97	↑0.96	↑0.96	↑0.98
6)	*r(L_A, V_{10m})*	**↗0.76**	**↗0.74**	**↗0.76**	**↗0.78**
7)	*r(L_A, V_{4m})*	→0.60	→0.62	→0.64	→0.65
8)	*r(L_A, $V_{1.5m}$)*	→0.57	→0.64	→0.62	→0.61
9)	*r(L_G, L_A)*	↑0.95	↑0.93	↑0.91	↑0.91
10)	*r(V_{hub},Power)*	↑0.98 (independent of measurement method)			
11)	*r(V_{hub}, V_{10m})*	↘0.37 (independent of measurement method)			
12)	*r(TS,Power)*	↑0.94 (independent of measurement method)			

Legend:

↑ - very strong correlation (|r|>0.9)

↗ - strong correlation (0.7≤|r|≤0.9)

→ - moderate correlation (0.4≤|*r*|<0.7)

↘ - weak correlation (0.2≤|*r*|<0.4)

To complement the correlation analysis, Figs. 9–12 show the temporal variability of L_G for the four microphone configurations using box plots for consecutive 10-min intervals.

The box plots present the median, interquartile range, whiskers and outliers for each interval.

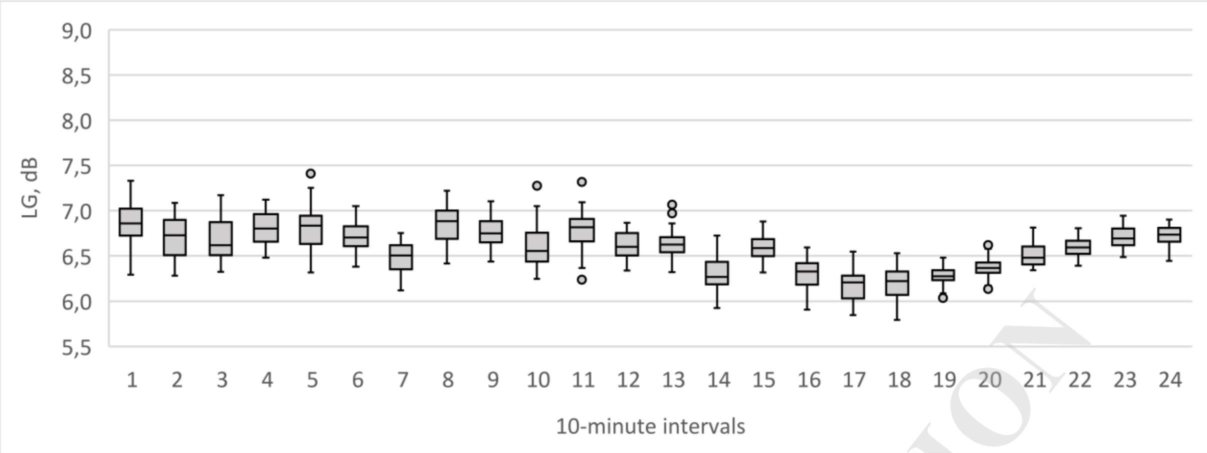

Fig. 9. Box plot of L_G for the 0m_DWS configuration.

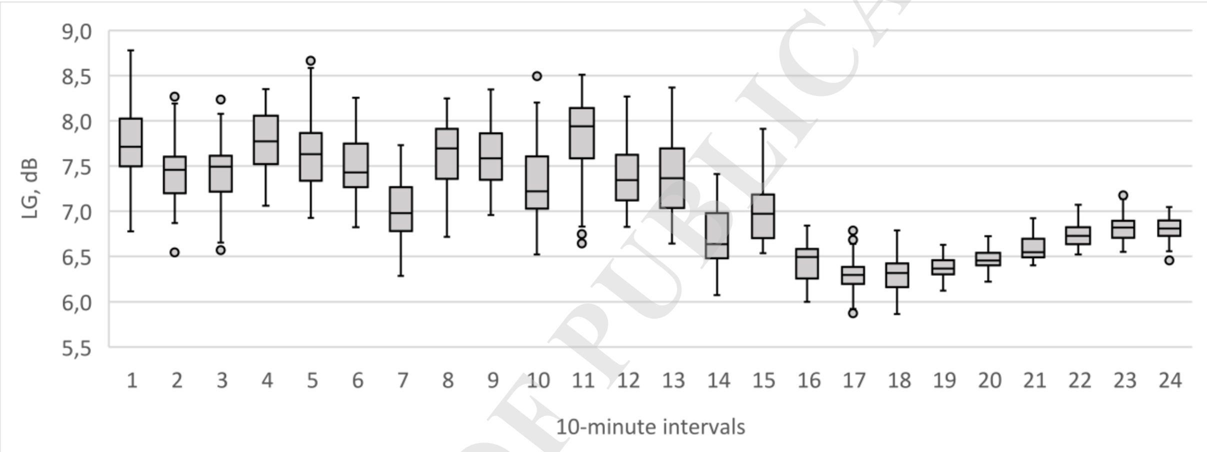

Fig. 10. Box plot of L_G for the 0m_SWS configuration.

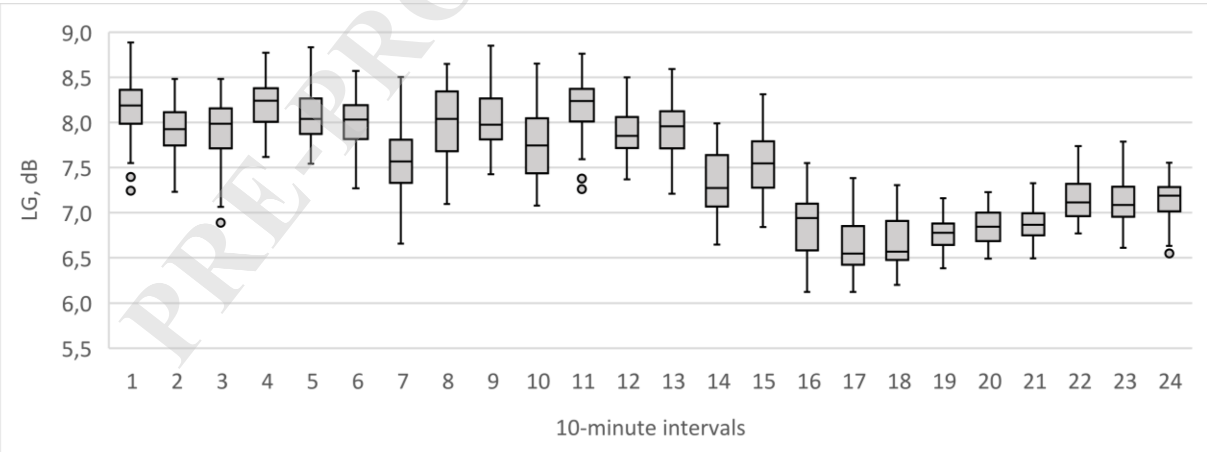

Fig. 11. Box plot of L_G for the 1.5m_SWS configuration.

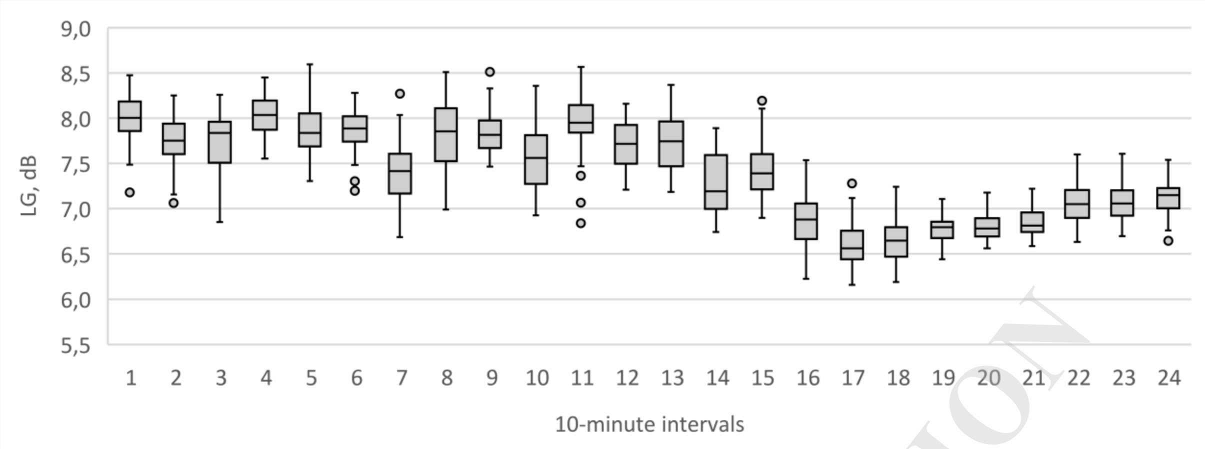

Fig. 12. Box plot of L_G for the 4m_SWS configuration.

5 Discussion

The results demonstrate that both microphone placement and windscreen configuration significantly affect the measured infrasound levels. Among the analysed configurations, the ground-plate setup with a double windscreen (0m_DWS) showed the highest resistance to wind-induced disturbances and the best agreement with turbine operation. This was reflected in the weak dependence of $L_G$on near-ground wind speed and its strong correlation with hub-height wind speed.

The remaining configurations (0m_SWS, 1.5m_SWS and 4m_SWS) were more sensitive to near-ground wind speed, resulting in higher $L_G$levels and greater dispersion. This is also visible in the box plots (Figs. 9–12): during intervals 1–13, when near-ground wind speed exceeded approximately 4.5 m/s, the 0m_DWS configuration showed the smallest interquartile range, whereas the single-windscreen configurations exhibited substantially higher variability.

During intervals 1–13/14, all turbines were operating and near-ground wind speeds were elevated, so both factors could contribute to increased dispersion. However, the relatively low variability of $L_G$for 0m_DWS indicates that near-ground wind, rather than the operation of additional turbines, was the main disturbance affecting the other configurations. This is supported by the high correlation between $L_G$for 0m_DWS and hub-height wind speed ($r(L_G, V_{hub}) = 0.96$), and by stronger correlations between tripod-mounted measurements and near-ground wind speed.

Limiting the number of operating turbines to one (intervals 18–24) enabled a clearer attribution of the recorded L_A and L_G sound levels to the test turbine alone. However, during this period, near-ground wind conditions also changed—the wind weakened considerably (from approx.

4.6 m/s during intervals 1–13 to 2.3 m/s during intervals 18–24), while wind speed at hub height remained similar (approx. 7 m/s and 13 RPM). This is clearly illustrated in Fig. 2–5. This means that the operating turbine emitted similar acoustic power in both periods, but with reduced wind interference in the near-ground layer. Under these conditions, the differences between microphone positions and windscreen types diminished, as lower wind disturbance made the microphone position and windshield effectiveness less critical.

This is particularly evident in Fig. 3 (and in Table 2A in the Appendix), where the L_G levels measured on the plate with single and double windscreens differ by only 0.7-1.5 dB at wind speeds of 2–2.5 m/s. In contrast, at higher wind speeds of 4.2–5.2 m/s (measured at 4 m height, intervals 1–13), the difference increased to 7.8–12 dB, with the lowest difference corresponding to the lowest wind speed (4.2 m/s, interval 7). This highlights the high sensitivity of the 0m_SWS configuration to wind speed, and conversely, the low sensitivity of the 0m_DWS configuration.

Also noteworthy is the difference between L_G levels measured on the plate and those recorded on tripods (1.5 m or 4 m). As seen in intervals 18–24, despite the low wind speeds, this difference still ranges from 2.8 to 5.7 dB. In intervals 1–13, with higher wind speeds, the difference exceeds 10 dB, reaching up to 15 dB in interval 1 (see Fig. 3 and Table 1A in the Appendix). It is important to remember that the tripod-mounted microphones were equipped only with single windscreens; therefore, the L_G levels measured in these configurations are significantly affected by wind noise, even at low wind speeds, as also demonstrated in [23].

Configurations with microphones mounted on a measurement plate (0m_DWS and 0m_SWS) showed greater consistency and stability in L_G results regardless of near-ground wind speed, in contrast to the tripod-mounted configurations (1.5m_SWS and 4m_SWS). This underscores the importance of placing the microphone close to the ground surface—even at low wind speeds (up to approx. 2.5 m/s). The 0m_SWS configuration, despite using the same windscreen as the tripod setups, exhibited noticeably better result stability due to its proximity to the ground, where wind disturbances are inherently lower.

Finally, the 0m_DWS configuration, additionally equipped with a secondary 500 mm windscreen, provided the highest measurement stability and immunity to near-ground wind interference, thanks to more effective suppression of wind gusts.

The use of Pearson correlation coefficients confirms their applicability for objectively assessing the degree of association between measured sound levels and turbine operating parameters.

Across all microphone placement configurations, a high correlation was observed between LG levels and wind speed at hub height, with an even stronger correlation for A-weighted sound levels (see Table 4). The strong correlation between LG and LA levels and wind speed at hub height confirms that LG is a reliable indicator of the turbine's operational state as a broadband and infrasound source. Notably, the 0m_DWS configuration demonstrated the highest agreement between L_G levels and turbine operating parameters under windier conditions.

Although L_A also exhibited a very strong correlation with hub-height wind speed across all configurations, it proved considerably less suitable for directly assessing turbine infrasound noise. As previously discussed, this results from the characteristics of the A-weighting filter, which strongly attenuates low frequencies—thereby eliminating a significant portion of the turbine-generated signal in the infrasonic and low-frequency range. Nevertheless, in this study, $L_A$is used only as an auxiliary diagnostic indicator rather than a metric of infrasound. When $L_A$follows turbine-related changes (e.g., with $V_{\mathrm{hub}}$and operating state) while $L_G$shows additional configuration-dependent variability, this suggests that $L_G$may be affected by wind-induced pseudo-noise and helps to interpret the reliability of the observed $L_G$trends in the infrasonic range.

The analysis of Fig. 2 and Fig. 3 also shows that wind speeds measured at different heights (e.g., 1.5 m, 4 m, and hub height) differ significantly. Wind speed at hub height directly affects the acoustic power radiated by the turbine, whereas LG measurements taken near the ground may be distorted by wind-induced pseudo-noise and local airflow turbulence around the microphone—an issue of particular relevance at the lowest frequencies.

These findings are consistent with the approach adopted in IEC/ISO 61400-11, which, for the purpose of measuring the sound power of wind turbines in the audible range, recommends the use of a ground-mounted measurement plate and appropriate windshields to reduce the impact of near-ground wind. Although this standard pertains specifically to sound power measurements in the audible frequency range, the present results confirm that the ground-plate approach with an enlarged windscreen can also improve the robustness of in-situ $L_G$assessment. At the same time, our measurements were conducted at a larger distance (250 m) than the IEC/ISO sound power geometry; therefore, we do not attempt to reconstruct incident-field levels or to derive a G-weighted sound power level from 0m_DWS. Consequently, the question of a generally reliable transfer function between $L_G$measured at ground level and elevated positions (1.5 m and 4 m) under environmental propagation conditions remains open.

6 Summary

The objective of the study was to evaluate the usefulness of selected microphone placement configurations and windscreen types (0m_DWS, 0m_SWS, 1.5m_SWS, and 4m_SWS), as well as acoustic indicators, for measuring infrasound noise generated by wind turbines. Particular attention was paid to the influence of microphone position and windscreen configuration on the stability (i.e., immunity to wind-induced disturbances) of infrasound noise measurements, represented by the G-weighted sound pressure level (L_G).

The most favourable results were obtained with the configuration using a microphone mounted on a ground measurement plate and equipped with a double windscreen (0m_DWS). This setup exhibited the lowest result variability and the strongest correlation with wind speed at hub height—a parameter directly related to the turbine's acoustic power output. At the same time, the weaker correlation with wind speed measured at 1.5 m and 4 m above ground confirms the setup's resistance to near-ground wind interference. This configuration, which is standard in sound power measurements according to IEC/ISO 61400-11, was also proven effective in environmental applications for infrasound noise assessment.

The correlation coefficient between L_G (measured in the 0m_DWS configuration) and wind speed at hub height was $r = 0.96$, while the correlation between hub-height wind speed and the turbine's electrical power output—directly related to its acoustic emission—was $r = 0.98$. These results confirm the high suitability of the L_G index, as measured in this configuration, for evaluating infrasound noise emitted by wind turbines—practically independent of near-ground wind conditions.

High correlation values between L_G levels and turbine operating parameters were also observed for the other microphone and windscreen configurations; however, their sensitivity to local wind disturbances was clearly greater. This was particularly evident for configurations with microphones placed at 1.5 m and 4 m, where, during intervals with stronger near-ground winds (1–13), L_G levels showed significant variability and higher values exceeding 85 dB in gust conditions (see Fig. 10–12), compared to values lower by several decibels measured on the plate using the 0m_DWS setup (Fig. 9). This confirms the high stability—and resistance to wind interference—of the 0m_DWS measurement configuration, even under relatively high near-ground wind speeds (4–5 m/s at 4 m height).

The findings provide a solid basis for methodological recommendations regarding environmental in-situ measurements of wind turbine infrasound, particularly with respect to the use of a ground-mounted microphone and enhanced wind shielding. Future research should focus on validating these observations under a wider range of meteorological and operational conditions and on further assessing the extent to which plate-based L_G measurements can support robust environmental infrasound evaluation.

Appendix

Table 1A. Average meteorological and turbine operational parameters for consecutive measurement intervals.

Interval	$V_{1.5m}$ *[m/s]*	V_{4m} *[m/s]*	V_{10m} *[m/s]*	V_{hub} *[m/s]*	*Wind direction*	*Temp. [°C]*	*Sun height [°]*	*Power output [kW]*	*Rotor speed [rpm]*
1	5.4	4.9	7.3	6.9	SE	9	31	534	13.1
2	5.5	4.8	7.1	6.8	ESE	9	30	581	12.9
3	5.0	4.6	6.3	7.5	ESE	9	29	701	13.8
4	5.5	5.1	6.6	6.8	ESE	9	28	547	12.9
5	5.6	5.2	6.6	7.1	SE	8	27	702	13.3
6	5.3	5.0	6.7	7.2	ESE	8	26	748	13.6
7	4.6	4.2	5.2	5.9	SE	8	25	313	11.5
8	4.7	4.4	5.8	6.7	SE	8	24	498	13.5
9	5.4	5.0	6.6	7.9	ESE	8	23	871	14.5
10	4.9	4.6	5.9	6.9	ESE	8	22	538	13.2
11	5.3	4.9	6.3	7.0	ESE	8	20	533	13.0
12	4.6	4.2	5.3	7.9	ESE	8	19	822	14.1
13	4.7	4.4	5.5	7.0	SE	8	18	626	13.3
14	3.5	3.2	4.4	6.6	ESE	8	17	464	12.5
15	3.5	3.2	4.7	6.5	ESE	7	15	424	12.2
16	2.6	2.4	3.6	5.9	SE	7	14	310	11.4
17	2.3	2.1	3.1	5.6	SE	7	13	252	10.7
18	2.5	2.2	3.1	5.7	ESE	7	11	283	10.8
19	2.2	2.0	3.5	5.9	ESE	6	9	301	11.1
20	2.5	2.3	3.4	6.4	ESE	6	8	388	12.1
21	2.3	2.0	3.2	7.2	SE	6	7	602	13.6
22	2.6	2.4	3.8	7.8	SE	5	5	814	14.5

23	2.8	2.5	4.0	7.9	ESE	5	4	872	14.6
24	2.7	2.5	3.8	7.4	ESE	5	3	703	14.5
BKG	2.6	2.5	3.8	8.0	ESE	5	1	847	14.6

Table 2A. L_G and L_A for consecutive measurement intervals and four microphone configurations.

Time interval	***L_G 0m DWS [dB]***	***L_G 0m SWS [dB]***	***L_G 1.5m SWS [dB]***	***L_G 4m SWS [dB]***	***L_A 0m DWS [dB]***	***L_A 0m SWS [dB]***	***L_A 1.5m SWS [dB]***	***L_A 4m SWS [dB]***
1	68.3	78.9	82.8	80.3	47.8	47.9	48.8	48.9
2	67.6	75.8	80.0	78.3	47.1	46.5	47.0	47.4
3	67.0	75.7	79.7	77.8	45.6	45.4	45.7	45.6
4	68.5	78.6	82.6	80.6	47.6	47.6	48.4	48.4
5	68.7	78.5	82.0	79.8	47.1	47.2	47.8	47.7
6	67.8	76.8	81.4	79.4	46.5	46.4	47.0	47.6
7	65.1	71.9	77.4	75.9	42.3	42.3	42.1	42.4
8	68.6	77.1	81.2	79.1	47.3	47.4	47.5	47.9
9	68.0	77.7	81.3	79.0	47.6	47.5	47.7	47.5
10	66.8	76.3	80.1	78.5	45.0	44.9	45.7	45.9
11	68.0	79.4	82.1	79.9	47.9	47.9	48.5	48.1
12	66.9	76.3	79.9	77.9	46.6	46.5	46.4	46.2
13	66.6	76.1	80.5	78.5	46.6	46.9	46.7	46.7
14	64.0	69.0	75.4	74.6	45.0	44.6	43.9	43.2
15	66.0	71.5	76.5	75.0	45.5	45.4	44.2	44.4
16	63.6	65.4	70.1	70.0	44.1	44.1	43.1	43.7
17	61.8	63.2	68.1	67.0	42.0	41.8	40.4	40.0
18	62.2	63.4	67.9	67.1	43.1	43.5	42.0	41.2
19	63.2	64.1	68.0	68.2	44.0	44.0	42.3	41.9
20	63.8	64.8	68.9	68.2	44.8	44.8	42.7	42.7
21	64.8	65.6	68.8	68.3	46.3	46.2	44.0	43.7

22	66.2	67.6	71.7	70.9	48.4	48.5	46.1	45.8
23	67.0	68.5	72.7	71.6	47.3	47.3	45.0	44.9
24	66.9	68.2	71.8	71.5	47.1	47.0	44.8	44.7
BKG	59.6	60.5	65.4	64.7	27.2	29.3	29.9	31.7
BKG 1	59.7	60.8	66.1	66.1	26.7	28.4	28.9	30.7
BKG 2	60.1	61.1	66.1	64.7	28.3	29.6	31.2	32.4
BKG 3	59.1	60.3	65.2	64.6	27.4	28.7	29.8	31.6

Funding

This research was funded by the National Centre for Research and Development – project No. NOR/POLNOR/Hetman/0073/2019 and by the Polish Ministry of Science and Higher Education – project No. 10 000-501.00-130 000.

Conflict of interest

The authors declare that there are no known competing financial interests or personal relationships that could have influenced the work described in this paper.

Authors' contributions

All authors contributed to the study conception, measurements, data analysis and manuscript preparation, and approved the final version.

References

[1] Baliatsas, C. *et al.* (2016) "Health effects from low-frequency noise and infrasound in the general population: Is it time to listen? A systematic review of observational studies," *Science of The Total Environment*, 557–558, pp. 163–169. Available at: https://doi.org/10.1016/j.scitotenv.2016.03.065.

[2] van den Berg, G.P. (2006) "Wind-induced noise in a screened microphone," *The Journal of the Acoustical Society of America*, 119(2), p. 824. Available at: https://doi.org/10.1121/1.2146085.

[3] Boczar, T. *et al.* (2022) "Measurement of Infrasound Components Contained in the Noise Emitted during a Working Wind Turbine," *Energies*, 15(2), p. 597. Available at: https://doi.org/10.3390/en15020597.

[4] Chiu, C.-H. and Lung, S.-C.C. (2020) “Assessment of low-frequency noise from wind turbines under different weather conditions,” *Journal of Environmental Health Science and Engineering*, 18(2), pp. 505–514. Available at: https://doi.org/10.1007/s40201-020-00478-9.

[5] Czapla, M. and Wszołek, T. (2024) “Experimental verification of the variability of amplitude modulation (AM) from wind turbines in relation to its assessment for annoyance,” *INTER-NOISE and NOISE-CON Congress and Conference Proceedings*, 270(3), pp. 8816–8833. Available at: https://doi.org/10.3397/IN_2024_4147.

[6] D’Amico, S., Van Renterghem, T. and Botteldooren, D. (2021) “Measuring infrasound outdoors with a focus on wind turbines: the benefits of a wind-shielding dome,” *Applied Acoustics*, 178, p. 108015. Available at: https://doi.org/10.1016/j.apacoust.2021.108015.

[7] Department of Trade and Industry (1996) *ETSU-R-97: The Assessment and Rating of Noise from Wind Farms*. London.

[8] Gaßner, L. *et al.* (2022) “Joint analysis of resident complaints, meteorological, acoustic, and ground motion data to establish a robust annoyance evaluation of wind turbine emissions,” *Renewable Energy*, 188, pp. 1072–1093. Available at: https://doi.org/10.1016/j.renene.2022.02.081.

[9] Hansen, C. and Hansen, K. (2020) “Recent Advances in Wind Turbine Noise Research,” *Acoustics*, 2(1), pp. 171–206. Available at: https://doi.org/10.3390/acoustics2010013.

[10] Hansen, K., Zajamšek, B. and Hansen, C. (2013) “Evaluation of secondary windshield designs for outdoor measurement of low frequency noise and infrasound,” *5th International Conference on Wind Turbine Noise Denver 28-30 August 2013* [Preprint].

[11] Hansen, K., Zajamsek, B. and Hansen, C. (2014) “Identification of low frequency wind turbine noise using secondary windscreens of various geometries,” *Noise Control Engineering Journal*, 62(2), pp. 69–82. Available at: https://doi.org/10.3397/1/376207.

[12] Hansen, K.L., Zajamšek, B. and Hansen, C.H. (2019) “Investigation of a microphone height correction for long-range wind farm noise measurements,” *Applied Acoustics*, 155, pp. 97–110. Available at: https://doi.org/10.1016/j.apacoust.2019.05.015.

[13] Hubbard, H.H. and Shepherd, K.P. (1990) “Wind turbine acoustics,” *NASA Langley Research Center*, pp. 153–183. Available at: https://doi.org/10.2495/978-1-84564-205-1/05.

[14] IEC 61400-11 (2018) “Wind turbines – Part 11: Acoustic noise measurement techniques.”

[15] Jakobsen, J. (2005) “Infrasound Emission from Wind Turbines,” *Journal of Low Frequency Noise, Vibration and Active Control*, 24(3), pp. 145–155. Available at: https://doi.org/10.1260/026309205775374451.

[16] van Kamp, I. and van den Berg, F. (2018) “Health Effects Related to Wind Turbine Sound, Including Low-Frequency Sound and Infrasound,” *Acoustics Australia*, 46(1), pp. 31–57. Available at: https://doi.org/10.1007/s40857-017-0115-6.

[17] Kłaczyński, M. and Wszołek, T. (2014) “Acoustic study of REpower MM92 wind turbines during exploitation,” *Archives of Acoustics*, 39(1), pp. 3–10. Available at: https://doi.org/10.2478/aoa-2014-0001.

[18] Leventhall, G. (2009) “Low Frequency Noise. What we know, what we do not know, and what we would like to know,” *Journal of Low Frequency Noise, Vibration and Active Control*, 28(2), pp. 79–104. Available at: https://doi.org/10.1260/0263-0923.28.2.79.

[19] Leventhall, G., Pelmear, P. and Benton, S. (2003) “A review of published research on low frequency noise and its effects,” *Department for Environment, Food and Rural Affairs (DEFRA)* [Preprint].

[20] Liebich, T. *et al.* (2022) “The effect of wind turbine noise on polysomnographically measured and self-reported sleep latency in wind turbine noise naïve participants,” *Sleep*, 45(1). Available at: https://doi.org/10.1093/sleep/zsab283.

[21] Møller, H. and Pedersen, C.S. (2011) “Low-frequency noise from large wind turbines,” *The Journal of the Acoustical Society of America*, 129(6), pp. 3727–3744. Available at: https://doi.org/10.1121/1.3543957.

[22] Müller, F.J.Y. *et al.* (2023) “Understanding subjective and situational factors of wind turbine noise annoyance,” *Energy Policy*, 173, p. 113361. Available at: https://doi.org/10.1016/j.enpol.2022.113361.

[23] Nguyen, P.D. *et al.* (2022) “Audibility of wind farm infrasound and amplitude modulated tonal noise at long-range locations,” *Applied*

Acoustics, 201, p. 109106. Available at: https://doi.org/10.1016/j.apacoust.2022.109106.

[24] Pohl, J., Gabriel, J. and Hübner, G. (2018) "Understanding stress effects of wind turbine noise – The integrated approach," *Energy Policy*, 112, pp. 119–128. Available at: https://doi.org/10.1016/j.enpol.2017.10.007.

[25] Preis, A. (2021) *Healthy society – towards optimal management of wind turbines' noise (HETMAN)*. Poznań.

[26] Raspet, R., Yu, J. and Webster, J. (2008) "Low frequency wind noise contributions in measurement microphones," *The Journal of the Acoustical Society of America*, 123(3), pp. 1260–1269. Available at: https://doi.org/10.1121/1.2832329.

[27] Rogers, A.L. and Manwell, J.F. (2004) *Wind Turbie Noise Issues*. Amherst.

[28] Rust, M. and Koch, C. (2024) "Performance comparison of measurement microphones and microbarometers for sound pressure measurements near wind power plants," *Journal of Low Frequency Noise, Vibration and Active Control*, 43(1), pp. 418–428. Available at: https://doi.org/10.1177/14613484231200852.

[29] Tachibana, H. (2014) "Outcome of systematic research on wind turbine noise in Japan," *Inter Noise 2014* [Preprint].

[30] Vestas Wind Systems A/S (2009) *Product brochure V90 1.8/2.0 MW*.

[31] Wszołek, T. *et al.* (2020) "Analysis of the Usefulness of Measurement on a Board at Ground Level for Assessing the Noise Level from a Wind Turbine," *Archives of Acoustics*, 45(1), pp. 165–175. Available at: https://journals.pan.pl/dlibra/publication/132492/edition/115760/content (Accessed: August 22, 2022).

[32] Wszołek, T., Mleczko, D., *et al.* (2022) "Experimental Verification of the Usefulness of Selected Infrasound and Low-frequency Noise (ILFN) Indicators in Assessing the Noise Annoyance of Wind Turbines," *Vibrations in Physical Systems*, 33(3).

[33] Wszołek, T., Pawlik, P., *et al.* (2022) "Experimental Verification of Windshields in the Measurement of Low Frequency Noise from Wind Turbines," *Energies*, 15(20), p. 7499. Available at: https://doi.org/10.3390/en15207499.